Fluid Phase Behavior Modeling of CO_2 + Molten Polymer Systems Using Cubic and Theoretically Based Equations of State

Pedro Arce,[1] **Martin Aznar,**[1] **Silvana Mattedi**[2]
[1] *School of Chemical Engineering, State University of Campinas, Campinas-SP, Brazil*

[2] *Chemical Engineering Department, Federal University of Bahia, R. Aristides Novis 2, Federação, 40210-630, Salvador-BA, Brazil*

Phase equilibrium data of CO_2 + molten polymer systems are of great relevance for chemical engineers because these are necessary for the optimal design of polymer final-treatment processes. This kind of processes needs information about gas solubilities in polymers at several temperatures and pressures. In this work, CO_2 solubilities in molten polymers were modeled by the perturbed chain-statistical associating fluid theory (PC-SAFT) equation of state (EoS). For comparison, the solubilities were also calculated by the lattice gas theory (LGT) EoS, and by the well-known Peng-Robinson (PR) cubic EoS. To adjust the interactions between segments of mixtures, there were used classical mixing rules, with one adjustable temperature-dependent binary parameter for the PC-SAFT and PR EoS, and two adjustable binary parameters for the LGT EoS. The results were compared with experimental data obtained from literature. The results in terms of solubility pressure deviations indicate that the vapor–liquid behavior for CO_2 + polymer systems is better predicted by the PC-SAFT model than by LGT and PR models. POLYM. ENG. SCI., 48:1157–1167, 2008. © 2008 Society of Plastics Engineers

INTRODUCTION

Solubilities of gases in molten polymers are of considerable importance in chemical engineering. Such data are of interest especially for the optimal design in polymer finishing processes, for instance, where the molten polymer is blanketed with inert gas; in certain specialized operations such as foam extrusion and fluidized-bed coatings; in the manufacture of polyvinyl chloride, etc.; and also when unreacted monomers exist in the polymerization products that are harmful to the environment and therefore devolatilization process is needed to remove them. All these processes need information about gas solubilities in polymers at various temperatures and pressures [1, 2]. To find the conditions met in the process design and operations, molecular thermodynamic models, such as equations of state, can be used to describe the gas–liquid equilibria [3].

In this work, two theoretically based equations of state: the perturbed chain-statistical associating fluid theory (PC-SAFT) EoS [4, 5] and the lattice gas theory (LGT) EoS [6, 7] and the well-known cubic PR EoS [8] are used to correlate gas solubilities in molten polymers. Classical mixing rules with one adjustable binary parameter, κ_{ij}, for the PC-SAFT and PR EoS, and two adjustable binary parameters, ${u_0}^{ma}/R$ and B^{ma}, for the LGT EoS, are used to measure the interactions between the segments of the mixtures. Satisfactory results have been obtained for PC-SAFT and LGT when compared with experimental data obtained from literature [1, 3, 9] and with those obtained by Peng et al. [2], who used their own equation of state.

THERMODYNAMIC MODELS

PC-SAFT EoS

The PC-SAFT EoS [4, 5] is based on a reference hard-sphere chain term and a perturbation contribution term,

$$\tilde{a}^{\mathrm{res}} = \tilde{a}^{\mathrm{hc}} + \tilde{a}^{\mathrm{pert}} \tag{1}$$

where $\tilde{a} = A/NkT$, and k is the Boltzmann constant. The hard-chain contribution [10, 11] is based on the first-order thermodynamic perturbation theory [12–14]:

$$\tilde{a}^{\mathrm{hc}} = \overline{m}\tilde{a}^{\mathrm{hs}} - \sum_{i=1}^{n_c} x_i(m_i - 1)\ln \mathrm{g}_{ii}^{\mathrm{hs}} \tag{2}$$

Correspondence to: Martin Aznar; e-mail: maznar@feq.unicamp.br
Contract grant sponsor: Fundação de Amparo à Pesquisa do Estado de São Paulo, FAPESP (Brazil); contract grant number: 05/53685-4; Contract grant sponsor: Conselho Nacional de Desenvolvimento Cientifico e Tecnológico, CNPq (Brazil); contract grant number: 150940/2005-0.
DOI 10.1002/pen.21069
Published online in Wiley InterScience (www.interscience.wiley.com).

where m is the segment number, x is the mole fraction and g_{ij}^{hs} is the radial pair distribution function which takes in account the interactions between molecules i and j, being defined as:

$$g_{ij}^{hs} = \frac{1}{(1-\xi_3)} + \left(\frac{d_i d_j}{d_i + d_j}\right)\frac{3\xi_2}{(1-\xi_3)^2} + \left(\frac{d_i d_j}{d_i + d_j}\right)^2 \frac{2\xi_2^2}{(1-\xi_3)^3} \quad (3)$$

and $\overline{m}$ is the arithmetic average of the segment number, calculated as:

$$\overline{m} = \sum_{i=1}^{n_c} x_i m_i \quad (4)$$

The hard-sphere contribution, $\tilde{a}^{hs}$, depends on the auxiliary variable ξ_k ($k = 0 \ldots 3$) and ξ depends on temperature-dependent segment number, d, and the total number density of molecules, ρ; thus:

$$\xi_k = \frac{\pi}{6}\rho \sum_{i=1}^{n_c} x_i m_i d_i^k, \quad k = (0,1,2,3) \quad (5)$$

where d_i is calculated as

$$d_i = \sigma_i[1 - 0.12 \cdot \exp(-3\varepsilon_i/kT)] \quad (6)$$

The perturbation contribution [15] is predicted from the first ($\tilde{a}_1$) and second-order ($\tilde{a}_2$) perturbation terms:

$$\tilde{a}^{pert} = \tilde{a}_1 + \tilde{a}_2 \quad (7)$$

where $\tilde{a}_1$ and $\tilde{a}_2$ depend on the total number density of molecules, ρ, the average of the segment number, $\overline{m}$, and the reduced density, η, and are expressed by classical van der Waals one-fluid mixing rules, represented as:

$$\tilde{a}_1 = -2\pi\rho\left(\sum_k^6 a_k(\overline{m})\eta^k\right)\sum_{i=1}^{n_c}\sum_{j=1}^{n_c} x_i x_j m_i m_j \left(\frac{\varepsilon_{ij}}{kT}\right)\sigma_{ij}^3 \quad (8)$$

$$\tilde{a}_2 = -\pi\rho\overline{m}\left(1 + Z^{hc} + \rho\frac{\partial Z^{hc}}{\partial\rho}\right)^{-1}\left(\sum_k^6 b_k(\overline{m})\eta^k\right) \times \sum_{i=1}^{n_c}\sum_{j=1}^{n_c} x_i x_j m_i m_j \left(\frac{\varepsilon_{ij}}{kT}\right)^2 \sigma_{ij}^3 \quad (9)$$

where

$$\left(1 + Z^{hc} + \rho\frac{\partial Z^{hc}}{\partial\rho}\right) = 1 + \overline{m}\frac{8\eta - 2\eta^2}{(1-\eta)^4} + (1-\overline{m})\frac{20\eta - 27\eta^2 + 12\eta^3 - 2\eta^4}{[(1-\eta)(2-\eta)]^2} \quad (10)$$

$$a_k(\overline{m}) = a_{ok} + \left(\frac{\overline{m}-1}{\overline{m}}\right)a_{1k} + \left(\frac{\overline{m}-1}{\overline{m}}\right)\left(\frac{\overline{m}-2}{\overline{m}}\right)a_{2k} \quad (11)$$

$$b_k(\overline{m}) = b_{ok} + \left(\frac{\overline{m}-1}{\overline{m}}\right)b_{1k} + \left(\frac{\overline{m}-1}{\overline{m}}\right)\left(\frac{\overline{m}-2}{\overline{m}}\right)b_{2k} \quad (12)$$

In the equations above, Z^{hc} is the hard-chain compressibility factor, whereas the constants a_{ik} and b_{ik} were fitted with thermophysical properties of pure n-alkanes [5]. Conventional combining rules are used to determine the cross parameters:

$$\sigma_{ij} = \frac{1}{2}(\sigma_i + \alpha_j) \quad \varepsilon_{ij} = \sqrt{\varepsilon_i \varepsilon_j}(1 - \kappa_{ij}) \quad (13)$$

where κ_{ij} is the parameter that regards the interactions between molecules i and j and m, σ and ε are the PC-SAFT pure-component parameters of each molecule.

LGT EoS

The equation of state used in this work was developed by Mattedi et al. [6, 7], and is based on the generalized van der Waals theory. It combines the Staverman-Guggenheim combinatorial term with an attractive lattice gas expression. A given fluid of volume V is represented by a lattice of coordination number Z_C (usually taken as 10) containing M cells of fixed volume V^*. Expressed as group contributions, the LGT EoS is given by:

$$Z = \tilde{v}r\ln\left[\frac{\tilde{v}}{\tilde{v}-1}\right] + \frac{Z_C}{2}\tilde{v}r\ln\left[\frac{\tilde{v}-1+(q/r)}{\tilde{v}}\right] + l - \frac{\tilde{v}\Psi(q/r)}{\tilde{v}-1+(q/r)}\sum_{i=1}^{n_c}\sum_{a=1}^{n_g} x_i v_i^a Q^a \frac{(\Gamma^a - 1)}{\tilde{v}-1+(q/r)\Gamma^a} \quad (14)$$

where Z is the compressibility factor, v_i^a is the number of groups of type a in a molecule of type i, Q^a is the area parameter of group a, and Ψ is an universal constant, taken as 1. The average number of segments occupied by a molecule in the lattice, r, the average number of close neighbors, q, and the reduced volume, $\tilde{v}$, are calculated by:

$$r_i = \sum_a v_i^a R^a \quad \text{and} \quad r = \sum_i x_i r_i \quad (15)$$

$$q = \sum_{i=1}^{n_c} x_i \sum_{a=1}^{n_g} v_i^a Q^a \quad (16)$$

$$\tilde{v} = \frac{V}{NrV^*} = \frac{v}{rv^*} \quad (17)$$

DOI 10.1002/pen

$$rV^* = \sum_{i=1}^{n_c} x_i \sum_{a=1}^{n_g} v_i^a V^a \tag{18}$$

$$rv^* = \sum_{i=1}^{n_c} x_i \sum_{a=1}^{n_g} v_i^a v^a \tag{19}$$

where R^a and V^a are the group-contribution parameters for the number of segments and hard-core volume, respectively; v^a is the parameter for the molar hard-core volume for a group of type a, and v^* is the cell molar volume, taken as 5.00 cm^3/mol. There are also other definitions:

$$\Gamma^a = \sum_{m=1}^{n_g} S^m \gamma^{ma} \tag{20}$$

$$S^m = \frac{\sum_{i=1}^{n_c} v_i^m x_i Q^m}{q} \tag{21}$$

$$\gamma^{ma} = \exp(-u^{ma}/(RT)) \tag{22}$$

where u^{ma} is the interaction energy between groups m and a. The fugacity coefficient for the model is:

$$\ln \hat{\phi}_i = -r_i \ln\left[\frac{\tilde{v}-1}{\tilde{v}-1+(q/r)}\right] + (1-l_i)\ln\left[\frac{\tilde{v}}{\tilde{v}-1+(q/r)}\right] + \frac{\Psi(q/r)(q_i-r_i)}{\tilde{v}-1+(q/r)} + \Psi\sum_{a=1}^{n_g} v_i^a Q^a \ln\left[\frac{\tilde{v}-1+(q/r)}{\tilde{v}-1+(q/r)\Gamma^a}\right] - \frac{\Psi}{r}\sum_{k=1}^{n_c}\sum_{a=1}^{n_g} x_k v_k^a Q^a \frac{\left(\sum_{e=1}^{n_g} v_i^e Q^e \gamma^{ea} - r_i\right)}{\tilde{v}-1+(q/r)\Gamma^a} - \ln\ Z \tag{23}$$

As suggested by Chen and Kreglewski [16], u^{ma} is represented by:

$$\frac{u^{ma}}{R} = \frac{u_0^{ma}}{R}\left(1+\frac{B^{ma}}{T}\right) \tag{24}$$

Thus, the EoS has four parameters for each group (v^a, Q^a, u_0^{aa}/R and B^{aa}) and two parameters for interactions between different groups (u_0^{ma}/R and B^{ma}). Because the influence of the temperature on the hard-core volume for several groups is quite low, a dependence function on temperature was not used for this parameter.

Peng-Robinson EoS

The Peng-Robinson (PR) EoS [8] can be written with the following form:

$$P = \frac{RT}{(V-b)} - \frac{a}{[V(V+b)+b(V-b)]} \tag{25}$$

The PR EoS parameters (a and b) are calculated with the following mixing rules:

$$a = \sum_i \sum_j x_i x_j a_{ij}; \quad b = \sum_i x_i b_i \tag{26}$$

The cross term, a_{ij}, is

$$a_{ij} = \sqrt{a_i a_j}(1-\kappa_{ij}) \tag{27}$$

where κ_{ij} is an adjustable parameter. The pure component parameters (a_i and b_i) are calculated from pure component critical properties:

$$a_i = 0.4572.\alpha_{(T_R)} \cdot (RT_{C,i})^2/P_{C,i}; \quad b_i = 0.0778RT_{C,i}/P_{C,i} \tag{28}$$

where $\alpha_{(T_R)} = [1+m(1-\sqrt{T_R})]^2$ and parameter m are defined in terms of acentric factor (ω), as

$$m = 0.3746 + 1.5423\,\omega - 0.2699\,\omega^2 \tag{29}$$

In this study, because polymers do not have critical properties, the energy and co-volume parameters of the pure polymer for the PR EoS, a and b, respectively, are obtained by fitting available pure liquid PVT data and assuming that parameters a/MW and b/MW are independent of MWs [17].

THERMODYNAMIC RELATIONSHIP TO DESCRIBE THE GAS–LIQUID EQUILIBRIA

The phase behavior for describing the gas-liquid equilibrium for gas + polymer mixtures at a fixed temperature can be modeled using the following equation [2]:

$$\hat{\phi}_2^L x_2^L = \phi_2^G \tag{30}$$

where x_2 and $\hat{\phi}_2^L$ are the solubility (mole fraction) and the fugacity coefficient of the gas in the molten polymer, respectively, ϕ_2^G is the fugacity coefficient of the pure gas at the same temperature and pressure of system.

PARAMETER FITTING

Carbon dioxide parameters were obtained by fitting vapor pressure and molar volume pseudo experimental data for saturated liquid from DIPPR correlation [18]. The polymer parameters were fitted using liquid volume pseudo experimental data at different pressures, computed with the Tait correlation [19]; for PBS and PBSA, the PVT data were taken from [20] over a pressure range suitable for engineering calculations. Detailed information about parameter fitting for each equation is reported in the following sections.

PC-SAFT EoS

The PC-SAFT pure-component parameters for the carbon dioxide were obtained by fitting vapor pressure and

molar volume data for saturated liquid [18] whereas the pure-component parameters for each polymer were obtained by fitting the liquid PVT experimental data [19, 20] over a pressure and temperature range suitable for engineering calculations using the modified maximum likelihood [21, 22] to minimize the objective function

$$\mathrm{OF} = \sum_{l}^{n_P} \frac{\left|P_l^{\exp} - P_l^{\mathrm{calc}}\right|}{P_l^{\exp}} + \sum_{l}^{n_P} \frac{\left|v_l^{\exp} - v_l^{\mathrm{calc}}\right|}{v_l^{\exp}} \quad (31)$$

The fitted characteristic parameters of each thermodynamic model were then used to calculate the average deviation of the specific volume,

$$\Delta v = \frac{1}{n_P} \sum_{l}^{n_P} \frac{\left|v_l^{\exp} - v_l^{\mathrm{calc}}\right|}{v_l^{\exp}} \quad (32)$$

where n_P is the pseudo-experimental data points, exp represents the volume values obtained from the Tait equation [19, 20] and calc represents the volume values obtained form the thermodynamic model.

The seeking method consisted of using an interval for each parameter to optimize [23] and, in this way, the search for the optimal pure-component parameters is performed over a wide interval of feasible solutions, of which just one satisfies the condition of the objective function. This method was used to predict the best parameters for the CO_2 and for the molten polymers.

LGT EoS

The carbon dioxide and the monomers were considered as groups, the co-monomer butylene succinate-*co*-butylene adipate was also considered as a group. Parameters for carbon dioxide were fitted using the Simplex as proposed by Nelder and Mead [24] to minimize the following objective function:

$$\mathrm{OF} = \left(\frac{\sum_k^{n_P} \left(\frac{VP_k^{\exp} - VP_k^{\mathrm{calc}}}{VP_k^{\exp}} \right)^2}{n_P} + 10 \left(\frac{P_C^{\exp} - P_C^{\mathrm{calc}}}{P_C^{\exp}} \right)^2 + 10 \left(\frac{T_C^{\exp} - T_C^{\mathrm{calc}}}{T_C^{\exp}} \right)^2 \right) \quad (33)$$

where VP is the vapor pressure, P_C is the critical pressure, and T_C is the critical temperature. The subscripts exp and calc mean experimental and calculated values, whereas n_P refers to the number of pure vapor pressure pseudo-experimental data points calculated with the DIPPR correlation [18]. In *Eq. 33*, a large weight was given to the deviations in critical properties, to better represent the high-pressure behavior of carbon dioxide. The critical temperature and pressure were calculated forcing the EoS to obey the critical conditions, which can be represented by:

$$\left(\frac{\partial P}{\partial \rho}\right)_T = \left(\frac{\partial^2 P}{\partial \rho^2}\right)_T = 0 \quad (34)$$

Polymer properties were computed by group contribution from their monomers. The polymer parameters were fitted using liquid volume pseudo experimental data at different pressures computed with the Tait correlation [19]; 400 points were used, evenly distributed in the temperature range of the correlation and in the pressure range from 1 bar to the higher pressure for the binary GLE data. A specific molecular weight was used for fitting, but the same group parameters can be used for any chain length formed by a monomer. As molecular weight, one of the experimental average molecular weights was used; if it was not reported, a molecular weight of 100,000 was used. The binary interaction parameters were fitted using least square deviation between calculated and experimental gas–liquid equilibria pressure.

PR EoS

The energy (a) and the co-volume (b) parameters of the pure polymer in the PR EoS are obtained by fitting available PVT data with a single set of (a/MW) and (b/MW) parameters for all MWs. The source of the required PVT data is the Tait equation, with the parameter values proposed by Rodgers [19]. These PR pure-component parameters for polymers were also obtained in a pressure and temperature range usually used in engineering calculations by using the minimization function shown in *Eq. (31)*. The critical properties for CO_2 were taken form DIPPR [18].

RESULTS AND DISCUSSIONS

In this work, the modeling of solubilities of CO_2 in several molten polymers is studied. Solubility pressure calculations are carried out for eleven polymers: HPDE, LDPE, i-PP, PVAc, PS, PMMA, PBMA, PDMS, PC, PBS, and PBSA in CO_2 in a range of temperature and at relatively high pressures, using two non-cubic and one cubic thermodynamic models, PC-SAFT, LGT, and PR EoS. The gas–liquid equilibrium experimental data were taken from literature, as shown in Table 1. This table also includes number of points, temperature and pressure ranges of the data and the adopted polymer molecular weight.

Evaluation of EoS Parameters for Pure Compounds

Pure-component parameters and the deviations from DIPPR correlation for carbon dioxide for each thermodynamic model are presented in Table 2. Just for compari-

 DOI 10.1002/pen

TABLE 1. Some physical properties of CO_2 + polymer systems used in this work.

Binary system: CO_2 +	n_P	T (K)	P (MPa)	MW polymer	References
HDPE	16	293.15–323.15	1.88–4.25	100,000	[25]
	17	433.15–473.15	6.608–18.123	111,000	[26]
LDPE	5	423.15	0.655–3.365	250,000	[27]
i-PP	5	453.15	7.083–17.242	220,000	[26]
	19	433.15–473.15	5.419–17.529	451,000	[26]
PVAc	49	313.2–353.2	0.294–10.100	100,000	[28]
	17	313.2–323.2	0.898–8.755	100,000	[29]
	31	313.15–373.15	0.199–17.449	100,000	[30]
PS	26	373.15–453.15	2.472–20.036	187,000	[31]
	6	298.15	0.400–0.900	50,000	[32]
	35	373.15–473.15	2.068–20.151	330,000	[30]
PMMA	77	263.15–453.15	1.520–9.120	100,000	[33]
PBMA	63	313.2–353.2	0.549–10.200	100,000	[28]
	8	298.15	0.200–0.900	13,600	[32]
PDMS	26	308.00	0.271–6.282	100,000	[34]
PC	7	293.15	0.992–5.836	100,000	[35]
	9	313.15–333.15	20.00–40.00	64,000	[36]
PBS	39	393.15–453.15	2.133–20.114	140,000	[37]
PBSA	37	393.15–453.15	2.079–20.127	180,000	[37]

son, the vapor pressure (VP) deviations were calculated using the following criterium:

$$\frac{\Delta VP}{VP} = \frac{1}{n_P}\sum_{i}^{n_P}\frac{\left|VP_i^{exp} - VP_i^{calc}\right|}{VP_i^{exp}} \tag{35}$$

where n_P represents the pseudo-experimental data points.

Vapor pressures are better predicted by the LGT EoS (its deviation is 0.42%) than the other equations; nevertheless, the other two equations predict it accurately: vapor pressures for CO_2 are correlated with deviations of 0.49% and 1.56% between DIPPR and PC-SAFT or PR, respectively. The results for LGT and PC-SAFT EoS are equivalent; however, the LGT equation has four parameters for each pure compound, whereas PC-SAFT has only three pure-component parameters and for the PR EoS it is used two pure-component parameters (T_C and P_C for the CO_2 and a/MW and b/MW for the polymer). Parameters for pure polymers and deviations from liquid PVT data obtained with the PC-SAFT, LGT, and PR models are presented in Tables 3–5, respectively. Liquid deviations from Tait pseudo-experimental data were calculated in a similar form of *Eq. (32)*. Liquid specific volumes were correlated by LGT with less than 0.47% deviation from Tait values for all polymers. This was the best results among the studied equations. However, PC-SAFT also correlates very well the liquid specific volume, with less than 1% deviation for all polymers, and PR EOS also satisfactorily correlates it, with less than 4% deviation for all polymers. The LGT equation is a lattice equation and correlate pure polymer liquid properties better than the other equations, because it is able to contabilize the structural characteristics in a best way for high molecular compounds.

TABLE 2. CO_2 pure-component parameters for the LGT and PC-SAFT EoS and critical properties for the PR EoS.

LGT EoS				
v^a (10^{-6} m^3/mol)	Q^a	B^{aa} (K)	u_0^{aa}/R (K)	ΔVP/VP (%)
22.256	3.7609	80.2794	−292.885	0.42
PC-SAFT EoS				
m/MW (10^{-3} kg/mol)$^{-1}$		σ (10^{10} m)	ε/k (K)	ΔVP/VP (%)
0.0482		2.7352	166.21	0.49
PR EoS				
T_c (K)	P_c (MPa)	ω		ΔVP/VP (%)
304.21	7.383	0.2236		1.56

Correlation of GLE Data

Table 6 presents the LGT, PC-SAFT and PR binary interaction parameters and the solubility pressure devia-

TABLE 3. Polymer pure-component parameters for LGT EoS.

Polymer	v^a (10^{-6} m^3/mol)	Q^a	B^{aa} (K)	u_0^{aa}/R (K)	$\Delta v/v$ (%)
HDPE	26.388	5.9511	71.9326	−585.115	0.028
LDPE	28.275	3.6613	430.459	−341.343	0.003
i-PP	38.334	7.7735	−34.7381	−728.592	0.067
PVAc	62.104	6.8088	534.043	−166.976	0.120
PS	87.004	9.2526	284.698	−284.711	0.034
PMMA	72.895	7.9554	308.326	−279.546	0.059
PBMA	99.329	21.641	888.962	−127.968	0.470
PDMS	59.942	9.8876	465.133	−262.826	0.040
PC	179.90	53.607	1109.24	−125.707	0.050
PBS	107.59	22.758	−30.4945	−644.193	0.034
PBSA	115.77	22.125	−32.7200	−676.791	0.043

TABLE 4. Polymer pure-component parameters for PC-SAFT EoS.

Polymer	m/MW (10^{-3} kg/mol)$^{-1}$	σ (10^{10} m)	ε/k (K)	$\Delta v/v$ (%)
HDPE	0.02819	4.0125	320.24	0.1879
LDPE	0.03391	3.7508	300.41	0.1704
i-PP	0.02453	4.2412	371.33	0.5967
PVAc	0.02991	3.5086	310.14	0.1298
PS	0.03324	3.5022	320.14	0.2845
PMMA	0.03408	3.3412	330.43	0.3542
PBMA	0.02616	4.0215	435.25	0.3815
PDMS	0.03252	3.5321	205.32	0.2812
PC	0.03719	3.1824	290.41	0.4215
PBS	0.05070	1.4932	411.37	0.5054
PBSA	0.02163	1.9911	399.36	0.9812

TABLE 5. Polymer pure-component parameters for PR EoS.

Polymer	a/MW (10^{-4} m^6 MPa/kg mol)	b/MW (10^{-6} m^3/mol)	$\Delta v/v$ (%)
HDPE	1.2795	1.2046	2.9512
LDPE	1.3698	1.1842	2.5845
i-PP	1.2875	1.2386	3.4256
PVAc	1.8412	0.8412	1.3341
PS	1.3052	0.9415	1.2548
PMMA	1.2647	0.8413	1.5236
PBMA	1.0215	0.9315	1.5635
PDMS	1.0148	0.9911	1.3841
PC	1.2815	0.5318	2.0153
PBS	1.4856	0.4842	3.9845
PBSA	0.2450	1.2817	3.4815

tions obtained in modeling CO_2 + polymer systems. In each case examined, the average absolute deviation in solubility pressure is reported, calculated from:

$$\frac{\Delta P}{P} = \frac{1}{n_P} \sum_{i}^{n_P} \frac{\left| P_i^{exp} - P_i^{calc} \right|}{P_i^{exp}} \tag{36}$$

where n_P represents of GLE experimental data points.

The PC-SAFT EoS is able to calculate satisfactorily the gas–liquid behavior for these systems, because the pressure deviations vary between 0.65 and 3.15%. For the LGT EoS, the deviations vary from 3.23 to 24.74%, whereas the deviations obtained with the PR EoS vary between 2.16 and 11.48%. In general, when higher pressures data (>15.0 MPa) are not used, a better fit is obtained.

The following comments summarize our observations on the obtained results. In general, the solubility of CO_2 in molten polymers usually decreases with increasing temperatures at constant pressure for many CO_2 + polymer systems, as it is shown through Figs. 1–10.

Correlated results and experimental data [25, 26] for the solubilities of CO_2 in molten HDPE at 433.15, 453.15, and 473.15 K are shown in Fig. 1. The isotherms have practically the same slope and the PC-SAFT and PR EoS are able to represent the fluid phase behavior of this binary system, while LGT EoS shows less accuracy. On the other hand, the fluid phase behavior of the LDPE (MW = 250,000) + CO_2 system was also modeled at 423.15 K using the PC-SAFT, LGT and PR EoS, and these results were compared with experimental data [27]. Lowest pressure solubility deviations correspond to PC-SAFT EoS (0.85%) whereas those obtained with the PR and LGT Eos were 2.16% and 3.23%, respectively.

Figure 2 shows the comparisons between calculated solubilities obtained by the three models and experimental data [26] at three temperatures for the CO_2 + i-PP systems. These three isotherms also have almost the same

TABLE 6. Binary interaction parameters for CO_2 + polymer systems using LGT, PC-SAFT, and PR EoS.

Binary system: CO_2 +	MW polymer	LGTY			PC-SAFT		PR	
		$B^{CO_2-polym}$ (K)	$u_0^{CO_2-polym}/R$ (K)	$\Delta P/P$ (%)	$\kappa_{CO_2-polym}$	$\Delta P/P$ (%)	$\kappa_{CO_2-polym}$	$\Delta P/P$ (%)
HDPE	100,000	−139.465	−706.379	24.74	0.0151	2.89	0.0186	6.15
	111,000			17.30	0.0103	3.15	0.0173	7.43
LDPE	250,000	295.062	−270.102	3.23	0.0084	0.85	0.0113	2.16
i-PP	220,000	69.623	−395.007	14.12	−0.0012	1.25	0.0215	6.18
	451,000			10.92	0.0008	1.38	0.0153	5.26
PVAc	100,000	115.878	−315.623	5.48	0.0035	0.89	0.0150	4.18
	100,000			9.99		1.02		3.16
	100,000			13.48		1.08		5.12
PS	187,000	74.823	−367.399	9.48	0.0063	0.78	0.0193	6.18
	50,000			13.43	0.0028	0.89	0.0216	8.11
	330,000			11.81	0.0065	0.85	0.0157	7.15
PMMA	100,000	170.621	−309.888	8.79	0.0103	0.85	0.0215	4.23
PBMA	100,000	380.242	−187.259	8.02	0.0084	0.95	−0.0099	4.83
	13,600			4.67	0.0025	0.92	0.0218	3.05
PDMS	100,000	261.946	−240.547	16.95	0.0153	1.06	−0.0118	7.43
PC	100,000	170.590	−361.489	17.35	0.0120	1.13	0.0126	11.48
	64,000			14.68	0.0138	1.05	0.0225	9.41
PBS	140,000	44.125	−397.228	3.54	0.0161	0.72	−0.0078	3.58
PBSA	180,000	60.468	−374.158	3.98	0.0183	1.25	−0.0107	6.40
Overall pressure deviations				11.16		1.21		5.87

DOI 10.1002/pen

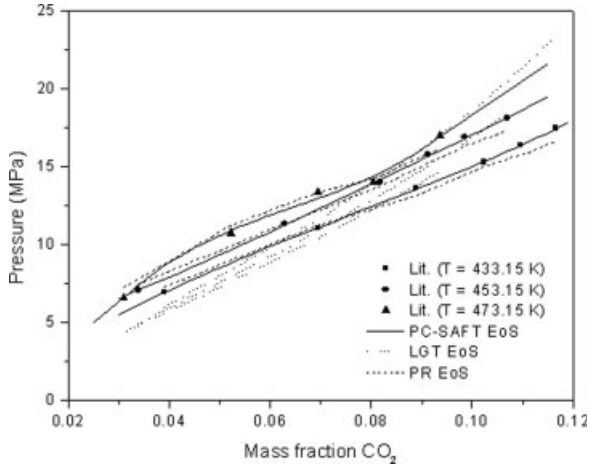

FIG. 1. Solubilities of CO_2 in molten HDPE (Experimental data were taken from Ref. 26).

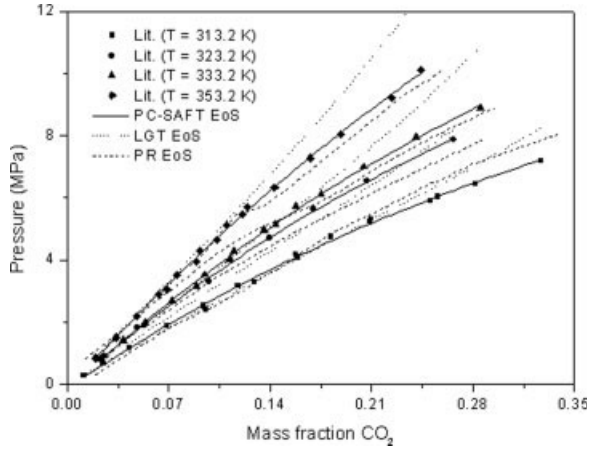

FIG. 3. Solubilities of CO_2 in molten PVAc (Experimental data were taken from Ref. 28).

slope, and PC-SAFT is able to correlate the data with more accuracy than LGT and PR EoS in terms of pressure solubility deviations. These pressure solubility deviations are 1.25% and 1.38% for PC-SAFT, 10.92% and 14.12% for LGT, and 8.18% and 10.26% for PR.

Correlated pressure solubilities obtained with the three thermodynamic models and the experimental data [28–30] at 313.2, 323.2, 333.2 and 353.2 K for the of CO_2 + PVAc system are shown in Fig. 3. These four isotherms join at lower CO_2 mass fractions, but at higher CO_2 mass fractions they seem to have the same slope. From this figure, it is clear that satisfactory results can be obtained with only one adjustable parameter for the PC-SAFT EoS; in the meantime, the LGT EoS obtains good accuracy at lower pressures, but when a pressure increased, its accuracy decreases. The same can be applied for the PR EoS, but with lower pressure solubility deviations than those obtained with the LGT EoS.

Figure 4 shows comparisons between calculated pressure solubilities and experimental data [30–32] at four temperatures for CO_2 + PS system. These four isotherms have different slopes. For instance, when temperature increases, the slope changes its inclination from horizontal to vertical. The PC-SAFT EoS can be able to correlate this binary system with higher accuracy than the LGT and PR EoS (0.78% to 0.89% in pressure solubility deviations for PC-SAFT against 9.48–13.4% for LGT and 6.18–8.11% for PR).

Correlated pressure solubilities of CO_2 in PMMA and experimental data [33] at seven temperatures are shown and compared in Fig. 5. From this figure, it can be noticed that at higher temperatures, the slopes of isotherms become more vertical and that the three models correlate this binary system with different accuracy. The LGT and PR EoS are less accurate at lower temperatures, whereas this accuracy increases at higher temperatures.

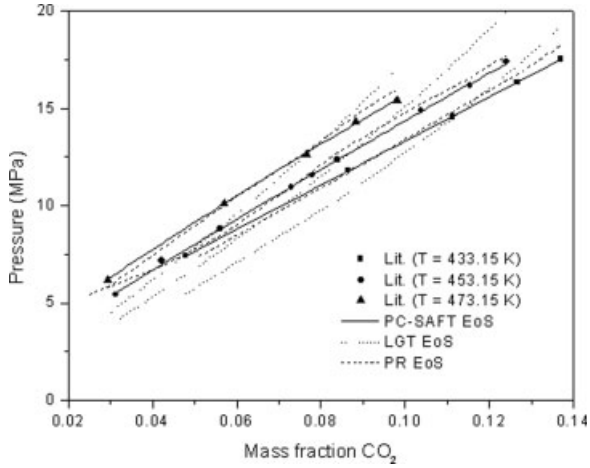

FIG. 2. Solubilities of CO_2 in molten i-PP (Experimental data were taken from Ref. 26).

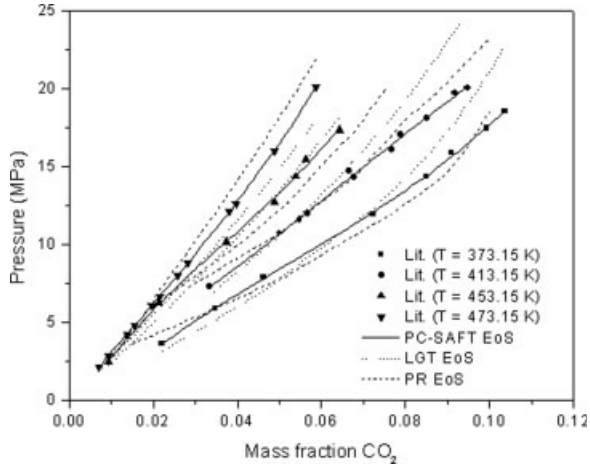

FIG. 4. Solubilities of CO_2 in molten PS (experimental data were taken from Ref. 30, 31).

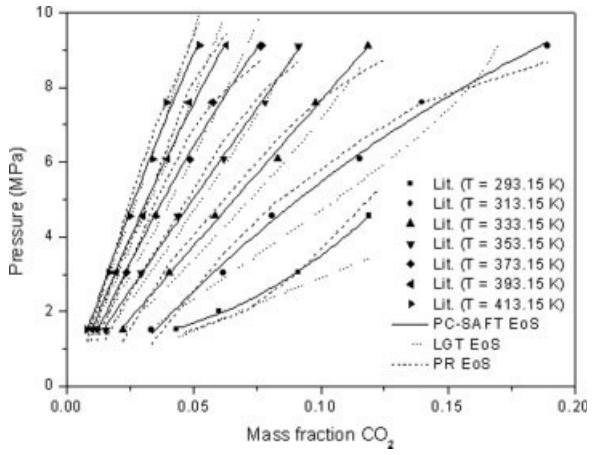

FIG. 5. Solubilities of CO_2 in molten PMMA (experimental data were taken from Ref. 33).

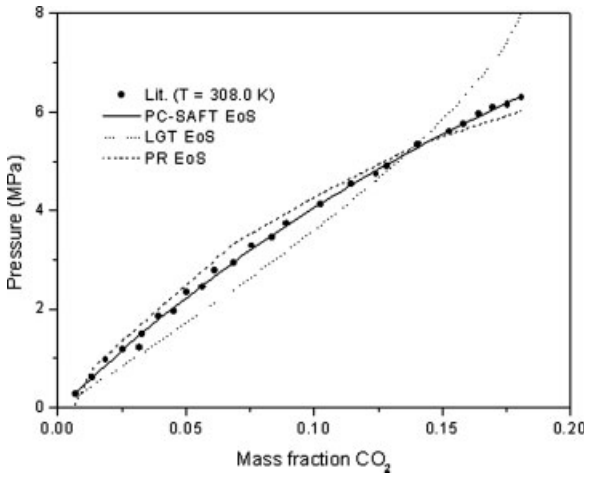

FIG. 7. Solubilities of CO_2 in molten PDMS (experimental data were taken from Ref. 34).

The PC-SAFT EoS can correlate this system with higher accuracy in terms of pressure solubility deviations (0.85%), whereas the deviations obtained with the LGT and PR EoS are 8.79% and 4.27%, respectively.

Figure 6 shows comparisons between calculated pressure solubilities and experimental data [28, 32] for CO_2 + PBMA system at 313.2, 333.2, and 353.2 K. These three isotherms join at lower CO_2 mass fractions and have different slopes at higher CO_2 mass fractions. Relative pressure deviations obtained for the PC-SAFT EoS are between 0.92 and 0.95%. Deviation values between 4.67% and 8.02% were obtained for the LGT EoS, whereas these values were between 3.05 and 4.87% for the PR EoS.

Figure 7 compares the calculated pressure solubilities obtained with the PC-SAFT, LGT and PR EoS with the experimental data for CO_2 in PDMS at 308.0 K [34]. From this figure, PC-SAFT has a better performance than the other two models. In terms of relative pressure deviations, the performance of each thermodynamic model was 1.06%, 16.95%, and 10.43% for PC-SAFT, LGT, and PR, respectively.

Correlated values and experimental data of the CO_2 + PC system [35, 36] at 313.15, 323.15, and 333.15 K are shown in Fig. 8. From this figure, it can be noticed that PC-SAFT is able to correlate the experimental data with higher accuracy, whereas LGT has a good performance just for 323.15 K; meantime, the PR EoS is also able to accompany the trajectory of the experimental data with less accuracy. In general, the relative pressure deviations obtained with the PC-SAFT, LGT, and PR EoS are 1.05% and 1.13%; 14.68% and 17.35%; and 9.41% and 11.48%, respectively.

Solubilities for CO_2 in PBS were studied in terms of pressure against CO_2 mass fraction at 393.15, 423.15, and 473.15 K. Experimental data [37] were modeled with the PC-SAFT, LGT and PR EoS. CO_2 mass fractions vary in

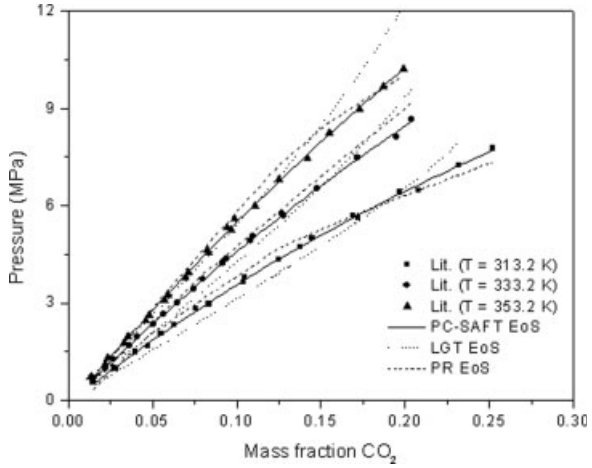

FIG. 6. Solubilities of CO_2 in molten PBMA (experimental data were taken from Ref. 28).

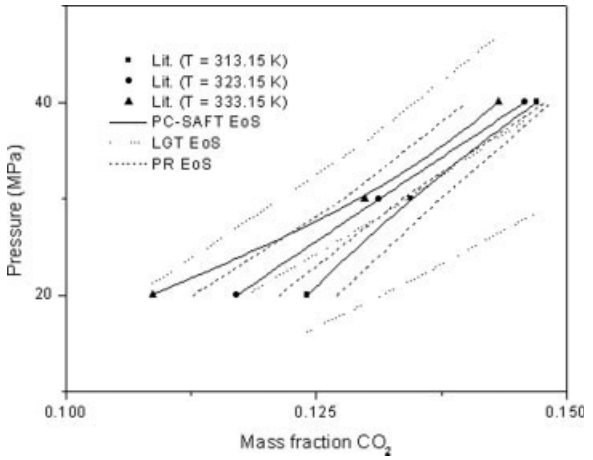

FIG. 8. Solubilities of CO_2 in molten PC (experimental data were taken from Ref. 36).

 DOI 10.1002/pen

almost linear form with the pressure at a given temperature, with the slope changing when temperature increases (see Fig. 9). The three models have a good performance in modeling this binary system; pressure solubility deviations obtained with PC-SAFT, LGT, and PR are 0.75%, 3.54%, and 3.68%, respectively.

Three isotherms originated for modeling the experimental data [37] of solubilities of CO_2 in PBSA with the three models are shown in Fig. 10. At all temperatures, the PC-SAFT EoS is able to model the fluid phase behavior of this binary system with more accuracy than the LGT and PR EoS. Pressure solubility deviations obtained with PC-SAFT, LGT, and PR are 0.65%, 3.98%, and 4.52%, respectively.

In a general way, the PC-SAFT EoS gives the best overall pressure deviation results, which is not surprising for polymer systems, because this thermodynamic model regards the monomer + monomer, monomer + solvent and solvent + solvent interactions in a rigorous form. Overall pressure deviations obtained by the LGT and PR EoS (11.16% and 5.87%, respectively) are higher than that obtained by the PC-SAFT EoS (1.21%). Surprisingly, the PR EoS predicts the vapor–liquid equilibria behavior for carbon dioxide + polymer systems better than the LGT EoS, although the latter predicts the pure polymer VLE behavior better. For mixtures, PR is much simpler than LGT and requires only one interaction parameter. These results indicate that, although LGT is able to correlate very well pure polymer systems, the mixture effects are not correctly predicted for highly asymmetric mixtures, such as CO_2 + polymer systems.

CONCLUSIONS

In this work, the pressure solubility of CO_2 in 11 molten polymers (HPDE, LDPE, i-PP, PVAc, PS, PMMA, PBMA, PDMS, PC, PBS, and PBSA) with different molecular weights was studied. For CO_2 + polymer systems, the solubility of CO_2 decreases when temperature increases at constant pressure. In terms of relative pressure deviations, the PC-SAFT EoS is able to model the phase behavior with highest accuracy than the LGT and PR EoS, even when it was used just one adjustable binary interaction parameter for the PC-SAFT and PR EoS and two adjustable interaction parameters for the LGT EoS.

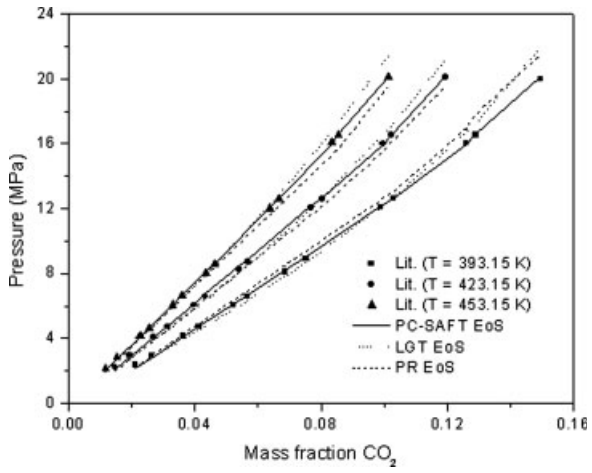

FIG. 9. Solubilities of CO_2 in molten PBS (experimental data were taken from Ref. 37).

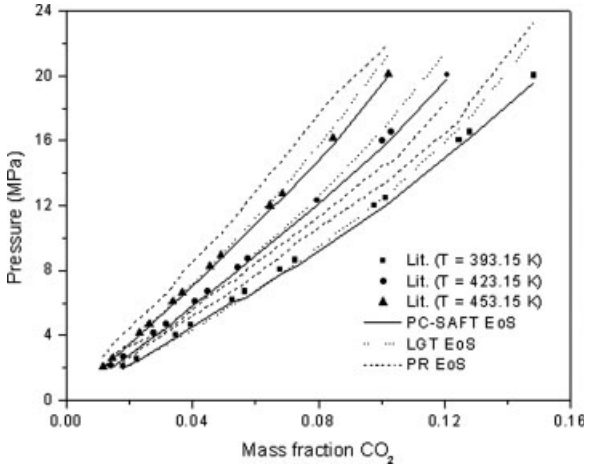

FIG. 10. Solubilities of CO_2 in molten PBSA (experimental data were taken from Ref. 37).

NOMENCLATURE

a	energy parameter for the PR EoS
$\tilde{a}$	Helmholtz free energy (dimensionless)
A	Helmholtz free energy
b	co-volume parameter for the PR EoS
B	adjust binary interaction parameter for the LGT EoS
d	temperature-dependent segment diameter
g	radial pair distribution function
k	Boltzmann constant
m	segment number, auxiliary parameter
$\overline{m}$	average segment number
MW	molecular weight
n	mole number
n_c	component number
n_g	number of segments
n_p	experimental point data
N	total number of molecules
P	system pressure
Pc	critical pressure
q	average number of close neighbors
Q	area parameter
r	average number of segments occupied by a molecule
R	ideal gas constant, group contribution parameter
T	absolute temperature
Tc	critical temperature

v	molar volume, number of groups, parameter for the molar hard-core volume, cell molar volume
$\tilde{v}$	reduced volume
V	volume, group contribution parameter
VP	vapor pressure
u_0	adjust binary interaction parameter for the LGT EoS
x	mole fraction
Z	compressibility factor
Z_C	coordination number

Greek Letters

Δ	pressure deviations
α	auxiliary parameter
ε	interaction energy parameter
$\hat{\phi}$	fugacity coefficient
η	reduced density
κ	adjustable binary interaction parameter for the PC-SAFT EoS.
π	constant
ρ	total number density of molecules; system density
σ	segment diameter
ω	acentric factor
ξ	auxiliary factor
Ψ	universal constant

Superscripts

a	segment group
calc	calculated
exp	experimental
G	gas phase
hc	hard chain
hs	hard sphere
L	liquid phase
pert	perturbation
res	residual
u	segment group

Subscripts

C	critical property
i,j	component
l,k	species
R	reduced property

Abbreviations

EoS	equation of state
GLE	gas–liquid equilibria
HDPE	high-density polyethylene
i-PP	i-polypropylene
LDPE	low-density polyethylene
LGT	lattice gas theory
PBMA	poly(buthylmethacrylate)
PBS	poly(butylene succinate)
PBSA	poly(butylene succinate-*co*-butylene adipate)
PC	polycarbonate bisphenol-A
PC-SAFT	perturbed chain-statistical associating fluid theory
PDMS	poly(dimethylsiloxane)
PMMA	poly(methylmethacrylate)
PR	Peng-Robinson
PS	polystyrene
PVAc	poly(vinyl acetate)
PVT	pressure - volume – temperature

REFERENCES

1. P.L. Durrill and R.G. Griskey, *AIChE J.*, **12**, 1147 (1966).
2. C.J. Peng, H.L. Liu, and H. Hu, *Chem. Eng. Sci.*, **56**, 6967 (2001).
3. N.H. Wang, S. Takishima, and H. Masuoka, *Int. Chem. Eng. (Japan)*, **34**, 255 (1994).
4. J. Gross and G. Sadowski, *Fluid Phase Equilib.*, **168**, 183 (2000).
5. J. Gross and G. Sadowski, *Ind. Eng. Chem. Res.*, **40**, 1244 (2001).
6. S. Mattedi, F.W. Tavares, and M. Castier, *Fluid Phase Equilib.*, **142**, 33 (1998).
7. S. Mattedi, F.W. Tavares, and M. Castier, *Braz. J. Chem. Eng.*, **15**, 313 (1998).
8. D.Y. Peng and D.B. Robinson, *Ind. Eng. Chem. Fundam.*, **15**, 59 (1976).
9. T. Hirose, K. Mizoguchi, and Y. Kamita, *J. Polymer Sci., Part B: Polymer Phys.*, **24**, 2107 (1986).
10. W.G. Chapman, G. Jackson, and K.E. Gubbins, *Mol. Phys.*, **65**, 1057 (1988).
11. W.G. Chapman, K.E. Gubbins, G. Jackson, and M. Radosz, *Ind. Eng. Chem. Res.*, **29**, 1709 (1990).
12. M.S. Wertheim, *J. Stat. Phys.*, **35**, 19 (1984).
13. M.S. Wertheim, *J. Stat. Phys.*, **35**, 35 (1984).
14. M.S. Wertheim, *J. Stat. Phys.*, **42**, 459 (1984).
15. J.A. Barker and D. Henderson, *J. Chem. Phys.*, **47**, 2856 (1967).
16. S.S. Chen and A. Kreglewski, *Ber Bunsen-Ges Phys Chem.*, **81**, 1048 (1977).
17. V. Louli and D. Tassios, *Fluid Phase Equilib.*, **168**, 165 (2000).
18. DIPPR Information and Data Evaluation Manager. Version 1.2.0, 2000.
19. P.A. Rodgers, *J. Appl. Polym. Sci.*, **48**, 1061 (1993).
20. Y. Sato, K. Inohara, S. Takishima, H. Masuoka, M. Imazumi, H. Yamamoto, and M. Takasugi, *Polym. Eng. Sci.*, **40**, 2602 (2000).
21. L. Stragevitch and S.G. d'Avila, *Braz. J. Chem. Eng.*, **14**, 41 (1997).
22. V.G. Niesen and V.F. Yesavage, *Fluid Phase Equilib.*, **50**, 249 (1989).
23. P. Arce and M. Aznar, *Fluid Phase Equilib.*, **238**, 242 (2005).

 DOI 10.1002/pen

24. J.A. Nelder and R. Mead, *Computer J*., **7**, 308 (1965).
25. N. von Solms, J.K. Nielsen, O. Hassager, A. Rubin, A.Y. Dandekar, S.I. Andersen, and E.H.J. Stenby, *J. Appl. Polym. Sci*., **91**, 1476 (2004).
26. Y. Sato, K. Fujiwara, T. Takikawa, S. Takishima, and H. Masuoka, *Fluid Phase Equilib*., **162**, 261 (1999).
27. P.K. Davis, G.D. Lundy, J.E. Palamara, J.L. Duda, and R.P. Danner, *Ind. Eng. Chem. Res*., **43**, 1537 (2004).
28. N.H. Wang, S. Takishima, and H. Masuoka, *Kogaku Ronbunshu*, **16**, 931 (1990).
29. S. Takashima, K. Nakamura, M. Sasaki, and H. Masuoka, *Sekiyu Gakkaishi*., **33**, 332 (1990).
30. Y. Sato, T. Takikawa, S. Takishima, and H. Masuoka, *J. Supercritical Fluids*, **19**, 187 (2001).
31. Y. Sato, M. Yurugi, K. Fujiwara, S. Takishima, and H. Masuoka, *Fluid Phase Equilib*., **125**, 129 (1996).
32. S. Wang, C. Peng, K. Li, J. Wang, J. Shi, and H.J. Liu, *Chem. Ind. Eng. (China)*, **54**, 141 (2003).
33. R.R. Edwards, Y. Tao, S. Xu, P.S. Well, K.S. Yun, and J.F. Parcher, *J. Phys. Chem. B*., **102**, 1287 (1998).
34. D.S. Pope, I.C. Sanchez, W.J. Koros, and G.K. Fleming, *Macromolecules*, **24**, 1779 (1991).
35. J.U. Keller, H. Rave, and R. Staudt, *Macromol. Chem. Phys*., **200**, 2269 (1999).
36. M. Tang, T.B. Du, and Y.P. Chen, *J. Supercritical Fluids*, **28**, 207 (2004).
37. Y. Sato, T. Takikawa, A. Sorakubo, S. Takishima, H. Masuoka, and M. Imaizumi, *Ind. Eng. Chem. Res*., **39**, 4813 (2000).